ELSEVIER

Journal of Nuclear Materials 257 (1998) 78–87

journal of nuclear materials

High magnification SEM observations for two types of granularity in a high burnup PWR fuel rim

N. Lozano [a], L. Desgranges [a,*], D. Aymes [b], J.C. Niepce [b]

[a] *C.E.N. Cadarache, F-13 108 St. Paul lez Durance, France*
[b] *Université de Bourgogne, UMR 5613 CNRS, Av. A. Savary, 21 011 Dijon, France*

Received 19 December 1997; accepted 26 March 1998

Abstract

Rim microstructure of an UO_2 pellet irradiated up to 61 GWd/tU, observed with high magnification scanning electron microscopy, presented two types of subgrains: polyhedral and round subgrains. Round subgrains were also observed on the surface of fabrication pores along the pellet radius. These round-shaped subgrains seem to be associated to free surface rearrangement. This new type of round subgrains was proved to be independent of the rim effect. Observations of the fuel structure in the vicinity of rim area evidenced two types of defects specific to rim effect: planar defects and small intergranular pores. Hypothesis is made that the accumulation of planar defects could generate polyhedral subgrains, a new description of the rim effect is proposed including this planar defect. These observations prove that a careful examination of subgrains morphology is necessary to identify rim effect.

PACS: 81.05.JE; 28.41.Bm

1. Introduction

The main aim in fuel technology is the search for improved economy, mostly through increased burnup. Therefore, studies on highly irradiated PWR fuel have been conducted in several countries and within the framework of international programmes (Halden, Risöe, HBEP,) [1–3].

At the end of the 1980s, with the development of the high burnup programmes, a phenomenon called the rim effect was identified at the pellet periphery when the fuel was irradiated beyond 60–70 GWd/tU local burnup. A comprehensive synthesis of the knowledge of the rim effect, and a mechanism proposal for the rim formation, was recently published by Hermitte [4] and Baron et al. [5].

The rim is characterised by numerous micronic faceted pores, submicronic grains coming from the subdivision of the initial grains, an increase of Pu and Nd concentration, and the Xe depletion seen by EMPA. The width of the rim can be determined by Xe depletion. Its thickness increases with burnup [4].

The influence of this new fuel morphology on thermal conductivity, fission gas release and pellet cladding interaction is still an open question. That is why a better understanding of this rim effect is needed.

To achieve progress in the characterisation and understanding of the rim effect mechanism, Scanning electron microscopy (SEM) observations at high magnification have been performed on a polished cross-section of a fuel pellet. A special care was given to fuel grain in the vicinity of rim effect. In this area, specific defects were observed that are described thereafter. Mechanism elements are then proposed which include these defects in rim formation.

2. Samples characteristics

Two UO_2 samples, with nominal enrichment of 4.5% of ^{235}U, were taken from two PWR fuel rods, J07 and

* Corresponding author. E-mail: desgrang@come.cad.cea.fr.

0022-3115/98/$ – see front matter
PII: S0022-3115(98)00056-7

Q02, with Zircaloy cladding, irradiated simultaneously in a EDF power reactor for five cycles. Table 1 gives the values of the mean linear power density for each cycles for J07. Pellets of 8.19 mm diameter, and 13.7 mm long exhibit a 10.45 density with a total porosity of 4.4%. Grain size varies from 12.2 μm at the pellet edge to 10.2 μm at the pellet centre.

Sampling was made at 800 mm from the bottom of the fissile column for J07, and 2212 mm from the bottom of the fissile column for Q02. The average local burnup was calculated to be 61 and 58.5 GWd/tU for J07 and Q02 respectively. The two slices obtained were polished up to a surface roughness of about 1 μm. Q02 sample was embedded in epoxy and chemically etched for ceramographic examination. J07 sample was embedded in metallic alloy with low boiling point, as required for electron probe micro-analysis. A part of J07 polished cross-section was damaged giving an area that can be considered as a fresh fractured one. Thus, it was possible to observe and compare fuel structure both with a polished surface and a fractured surface.

In a first stage, electron probe micro-analysis (EMPA) was performed on J07 sample to study fission product radial evolution, and their implantation inside the internal zirconia (Fig. 1). Rim width determined by Xe depletion zone (i.e. when the measured concentration becomes lower than the calculated one) was estimated to be about 200 μm (Fig. 2(a)). The porosity distribution was determined by image analysis excluding fabrication pores [6]. It appears that the number of small pores, characteristic of the rim area, increases from 200 to 5 μm from the pellet edge. It is correlated with the Xe depletion in the rim region (Fig. 2(b)). The corresponding results will be detailed in a forthcoming paper [6].

New SEM characterisations were performed with a SEM Philips XL30 on J07 sample. Despite the shielding, it was possible to work at high magnification. Q02 sample, chemically etched, was characterised by optical metallography.

For the sake of clarity, experimental observations are grouped in three paragraphs, namely, rim granularity, rim porosity and expanse of the restructured area. Interpretation of rim phenomenon is then discussed.

3. Rim granularity

In a fractured area of sample J07, typical granularity of rim area is emphasised on Figs. 3 and 4. In Fig. 3 the existence of two types of subgrains is clearly evidenced. Polyhedral subgrains, with a size of 0.5–0.8 μm, are characterised by bright lines that can be attributed to sharp ridges. Round subgrains, with no such bright lines, 0.1 μm in size, are essentially located around pores with micronic sizes.

Table 1
Linear power values for each irradiation cycle for J07

Cycle	1	2	3	4	5
Linear power, W cm^{-1}	220	270	230	190	170

Fig. 4 taken at 50 μm from the pellet edge, in the fractured region of the sample and at the bottom of a big pore, illustrates two different morphologies: on the left side of the photo, round subgrains only appear at the grain surface on the inside of a fabrication pore, whereas on the right side, a more classical morphology of the rim area fractured surface is observed. These observations clearly exhibit two different types of granularity in the rim area. Polyhedral and round subgrains are indeed different considering their shape and their size. Round subgrains, because they seem to be correlated to pores, will be discussed in next paragraph with an examination of the inside of fabrication pores along a pellet radius. Polyhedral grains are discussed now.

3.1. Polyhedral subgrains

They are observed only inside the rim area, and thereby are characteristic of this effect. Polyhedral subgrain shape suggests that these grains are bounded by crystallographic planes. As proposed by Une et al. [2] and Thomas et al. [7], these planes can be domain walls, which separate recrystallized material and high concentration defect regions. They could also be correlated to planar defects observed in fuel grains surrounding rim area.

Planar defects are evidenced in Fig. 5, which is a ceramography of Q02 chemically etched sample, showing from top to bottom, cladding, internal corrosion layer, rim area and fuel grain in its vicinity. Grains are marked with small sticks, a few micrometers long, regularly arranged along two or more directions. Sticks density on fuel surface increases when reaching pellet edge, i.e. when increasing burnup. Some authors interpreted these sticks as a circular phases deriving from fuel oxidation and U_4O_9 formation [8]. However, measurement of fuel oxygen potential [9] tend to prove that rim area is near to stoechiometry, and up to now no experimental evidence has been given for fuel oxidation.

These sticks could also be similar to a planar defect already mentioned by Thomas et al. [7]. Using TEM on irradiated fuel with average burnup of 48 GWd/tM, they evidenced plate shaped defects, approximately 0.5 μm in diameter and 0.05 μm thick. They suggested, from the hollow interior and surrounding dislocation tangles, that the defect may have formally contained gases at high pressure. Similar defects, up to several micrometers in diameter and having {1 1 1} crystallographic habit planes were previously observed in a lower burnup fuel by the same team [7]. The authors claimed that despite a

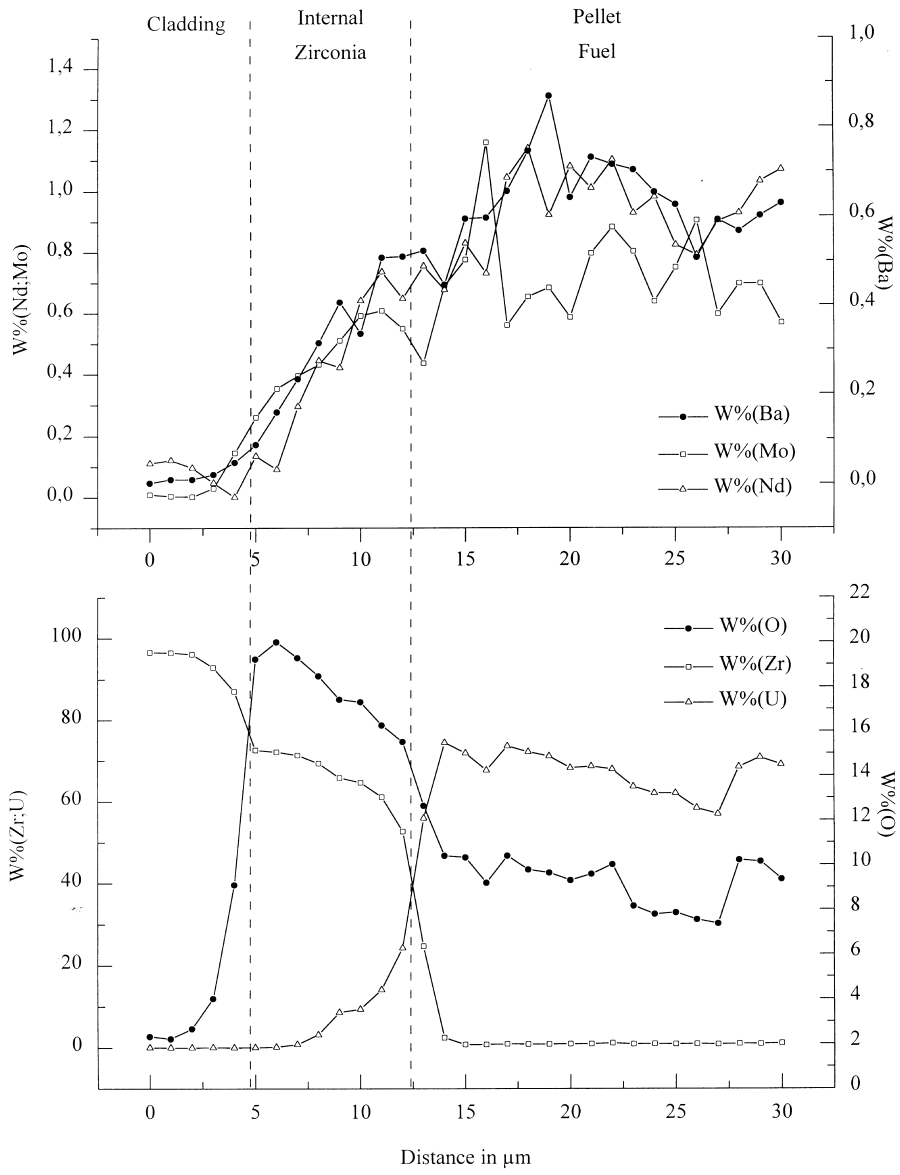

Fig. 1. EPMA fission product profile at the fuel to clad interface.

superficial resemblance to U_4O_9, these defect contained no detectable U_4O_9 or higher uranium oxide phases.

An equivalence between sticks observed on ceramography and plate shaped defects could be deduced from the fact sticks are neither seen directly on ceramography, nor by ionic etching, but only by chemical etching. Thickness of plate shaped defect makes them undetectable by optical ceramography. Ionic etching provide a uniform erosion on a grain surface, and keep the same thickness of defect. On the contrary chemical etching round defect edges, which makes them thicker and visible.

It is then possible to make the hypothesis that sticks and plate shaped defects are a unique type of planar defect. This planar defect would create two free surfaces along a crystallographic plane inside a grain. These planes might be the faces of rim subgrains and explain their polyhedral shape.

3.2. Round subgrains

Because round subgrains seem to be correlated to pores surface, an examination of grain surface was performed on the inside of fabrication pores revealed by

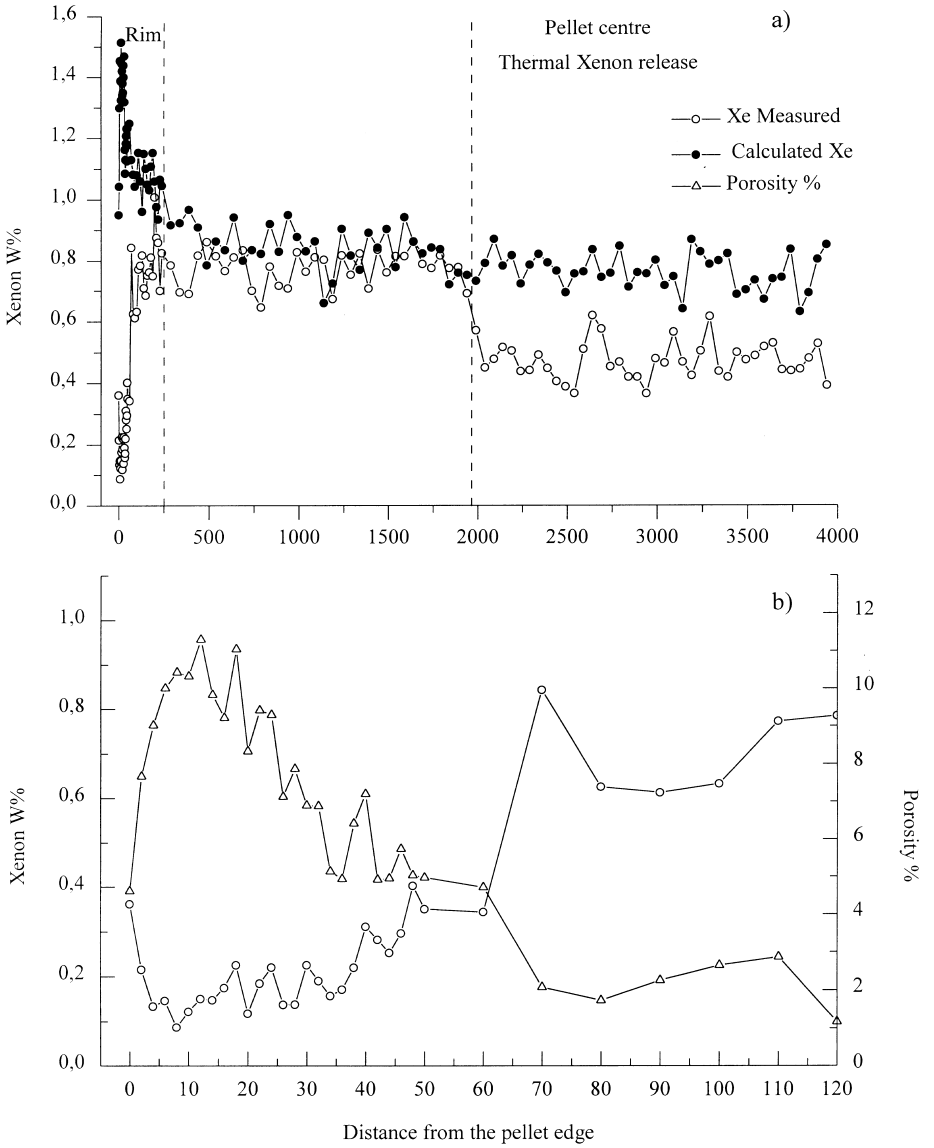

Fig. 2. Xenon concentration (wt %) on the matrix and porosity density, versus radius (μm).

polishing, all along a pellet radius. A specific evolution of surface morphology is illustrated in Figs. 6–8. Fig. 6(a) illustrates the three types of surface morphology that can be observed from pellet centre to 500 μm from pellet edge. In pellet centre, grains surfaces are plane, dotted with 0.1–0.3 μm pores. Grains can also exhibit surfaces with stairs 0.7 μm thick, that can be viewed as a succession of hills and valleys along one direction. The third surface morphology consists of a two-dimensional array of hills and valley defining 0.3–0.6 μm rectangular subgrains. The arrangement of the subgrains follows a very regular pattern, as shown in Fig. 6(b) which is a detail of Fig. 6(a).

Only two dimension ordered surfaces are observed while getting close to the pellet edge. At 200 μm from the pellet edge (Fig. 7), subgrain shape becomes more spherical. Inside rim area (Fig. 8), at 150 μm from the cladding, it becomes clear that the ordered pattern disappears leaving room for a random distribution of round subgrains. Moreover, the grain size decreases when approaching the pellet outer surface, as summarised in Table 2.

Similar features have already been observed on a fractured cross-section of CANDU fuel [10]. The grain surface presents rearrangement even if the irradiated fuel has a low burnup and a natural initial ^{235}U concentra-

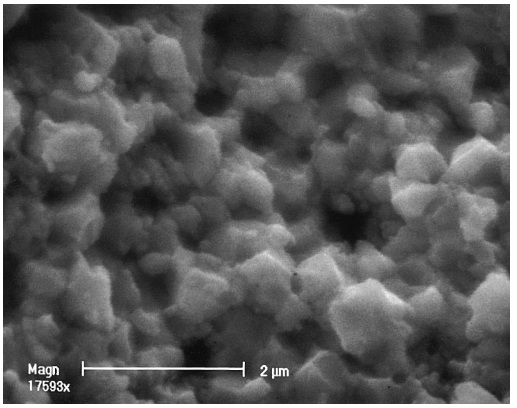

Fig. 3. SEM high magnification observation of the fractured rim: round and polyhedral subgrains are pointed out.

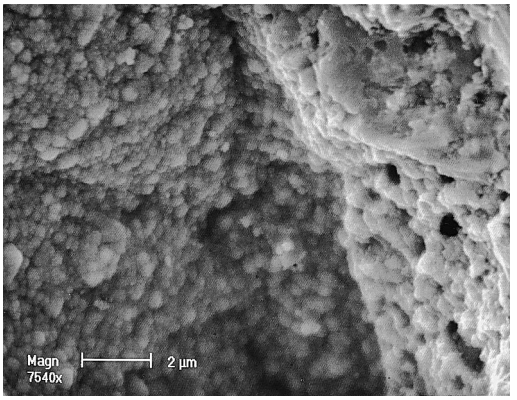

Fig. 4. At 50 μm from the pellet edge, the fabrication pore on the left presents disordered round subgrains, and on the right, the fractured fuel presents rim subgrains and pores.

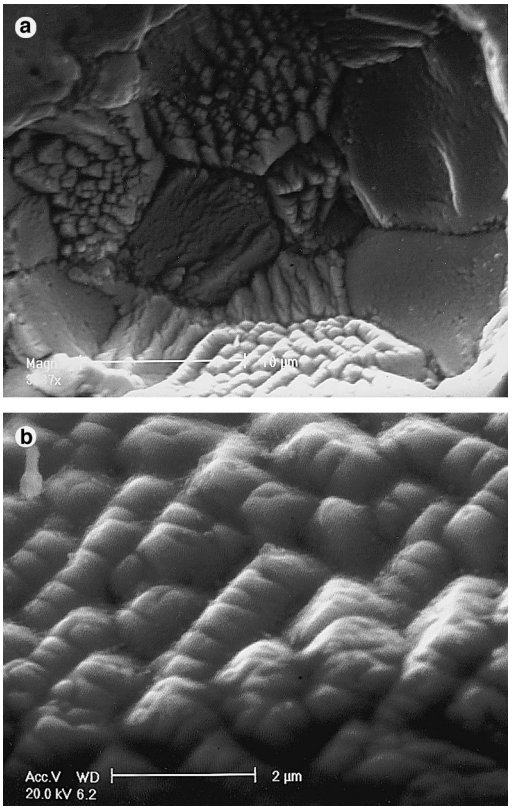

Fig. 6. (a) Locate the figure (b) at 500 μm from the pellet edge, on a fabrication pore, grain surface subdivision into rolls, at fabrication pore bottom.

tion [10]. Rolls or round subgrains observed are arranged on the grain surface, with 0.3–0.7 μm size. But this scanning of fractured CANDU fuel does not allow to locate subgrains.

Our observations tend to prove that surfaces subdivided on round subgrains are associated with open

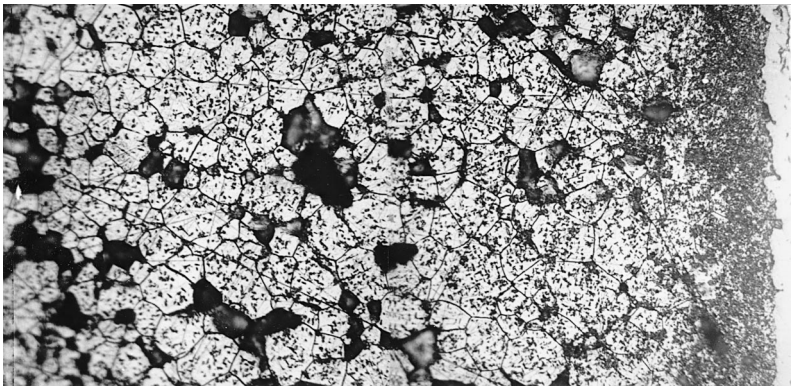

Fig. 5. Planar defects evidenced on a mettallographic observation of Q02 sample.

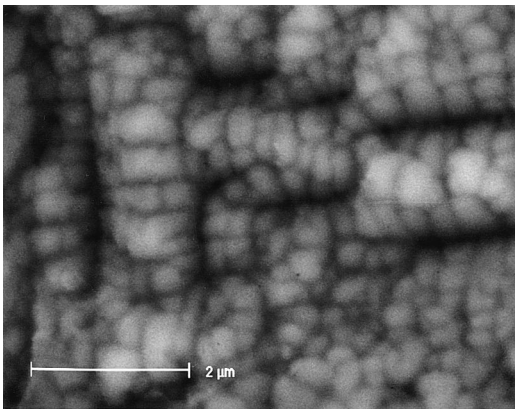

Fig. 7. At 200 μm from the pellet edge, on a fabrication pore, grain surface subdivision on rolls, which are subdivided on ordered round subgrains.

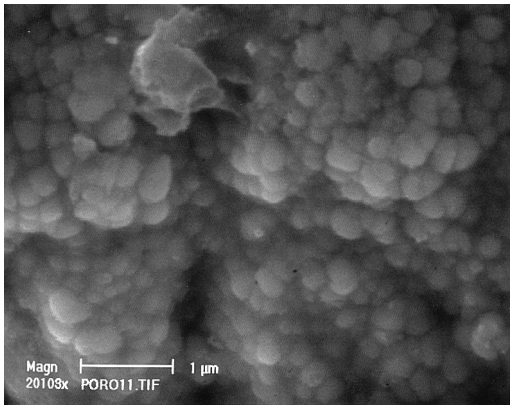

Fig. 8. At 150 μm from the pellet edge, disordered round subgrains on a fabrication pore.

surfaces on initial pores. Furthermore this fragmentation phenomenon is not correlated to the rim effect. First, CANDU fuel burnup is too low to allow the appearance of the rim [1,10]. Second, on our samples, round subgrains exist in areas as far as 2000 μm from pellet edge while the rim effect is only observed up to 200 μm from the pellet edge. Third, their morphology is very different from the rim morphology illustrated by Fig. 4.

Round subgrain size decrease while getting closer to pellet edge could be associated to the temperature profile in the pellet rather than to the burnup evolution. A specific mechanism will be proposed in a next section to describe round subgrains formation and evolution on pores surfaces.

From the above considerations, we can assess that round subgrains seen in rim area are not specific to rim effect. They only appear because of creation of pores due to rim effect. To obtain a more precise idea on the relation between porosity and rim effect, a study of porosity evolution with the rim effect has been conducted and is presented in the following paragraph.

4. Rim porosity

The rim effect is also characterised by small pores, in the size range of 0.5–1 μm. To study either any correlation could exist between planar defects and pores formation, small pore evolution has been observed on J07 sample polished surface from 1000 μm to the pellet edge.

From 1000 to 400 μm from the pellet edge, pores seem to be intergranular: small pores are scattered and separated by compact ceramic which could correspond to initial grains. Sometimes, these pores are linked and form a chain of pores. Between the rim area and 400 μm from the pellet edge, scattered pores are observed inside original grains.

Fig. 9 (280 μm from the pellet edge) illustrates these types of pore distribution. An initial grain is surrounded by intergranular pores, on the left side of Fig. 8 these are separated, but on the right side they are so close that a long and narrow pore is formed. Initial grains, rounded by intergranular pores, also present an intragranular porosity. In the rim region, pores are so numerous that intragranular pores cannot be distinguished from the intergranular ones.

Several studies [11,12] show that fission gas release and pore formation are correlated. Xe concentration profile and the curves of pore area rate are presented in Fig. 2 [6]. The correlation between the two curves suggests that pores are filled with fission gases, and emphasises the hypothesis of pore gas origin.

Due to their radial position on the pellet, these pores exist at a lower burnup than 60–70 GWd/tU, which is considered to be a threshold for the appearance of grain subdivision in the pellet edge [1]. However they can be considered as correlated to the rim phenomenon, be-

Table 2
Grain open surface observation on fabrication pores

Distance from the pellet edge in μm	0–50	150	200	500–2000
Rolls or subgrain size in μm	0.1	0.2–0.5	0.3–0.7	0.7
Observations	Disordered round subgrains	Disordered round subgrains	Ordered round subgrains	Ordered rolls

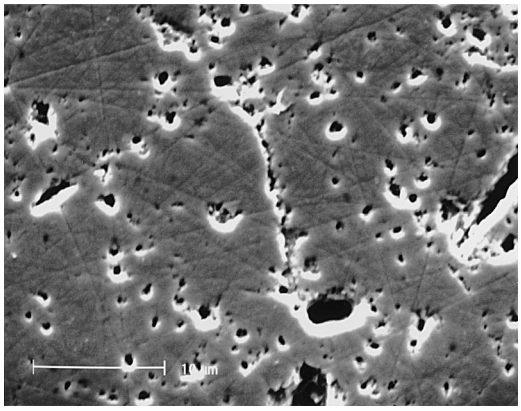

Fig. 9. At 280 μm from the pellet edge, arrangement of small pores formed during irradiation. An initial grain, rounded by intergranular pores, present an intragranular pore in its centre.

cause their density increases when getting closer to the pellet edge.

With these present SEM observations, the porosity correlated to the rim phenomenon can be characterised first by the appearance of intergranular pores, which can form long and narrow pores at the grain boundaries, and then by the appearance of intragranular pores. Because pore apparition and planar defect seem to be linked to rim effect and appear before the burnup threshold usually accepted for rim formation, it sounds reasonable to associate them in the same mechanism for rim formation. Some elements of this mechanism will be presented in a further chapter.

5. Expanse of the restructured area

Pores and subgrains formation affect the original grain forming what will be called restructured area. Optical ceramography would lead to the conclusion that fuel is totally restructured in rim MEB observations on the polished surface of J07 sample provide a more precise description.

Because of polishing restructured area can be revealed. A diamond paste grade of 2 μm indeed was used for the last polishing step. Small subgrains, as seen in the rim area, cannot be polished in this last step because they are smaller than the diamond paste grains (this interaction is better described as grinding). So, the surfaces where submicronic grains exist are not flat, but reveal some roughness. The surface of restructured areas increases from 60 to 5 μm from the pellet edge and some polyhedral submicronic grains are observed in these regions.

On the contrary, the flat surfaces observed in the rim area should be considered as part of unrestructured fuel. Unrestructured parts, bounded by pores and ruined areas, are large at 100 μm, and small and discreet at 10 μm from the pellet edge. This is illustrated in Fig. 10, in which the rim area from 30 μm to the pellet edge is presented. Oxidised cladding or internal zirconia is characterised by its dark colour on the left side.

Unrestructured areas and polyhedral subgrains are also observed differently in the rim area on fractured and on polished material. Fig. 11 shows that intact material parts, observed on the polished rim in the right side of photo, are not revealed on the fractured surface.

These observation would mean that the subdivision process is not totally completed as claimed in Ref. [3]. This difference in interpretation can arise from the difference in observed material. On fractured surfaces, intact grains are less likely to be seen, because fractures generally propagate along mechanically weak zones, i.e. in the case of the rim, where subgrains and porosity exist. This effect should be even greater when long intergranular porosities exist. This is clearly evidenced in Fig. 10.

The five peripheral micrometers of the fuel are made of compact material, with few or no pores. The contact region between cladding and fuel is unrestructured, as shown on the left of Fig. 10. This interface shows other morphologies, as in Fig. 12, where an important inter-

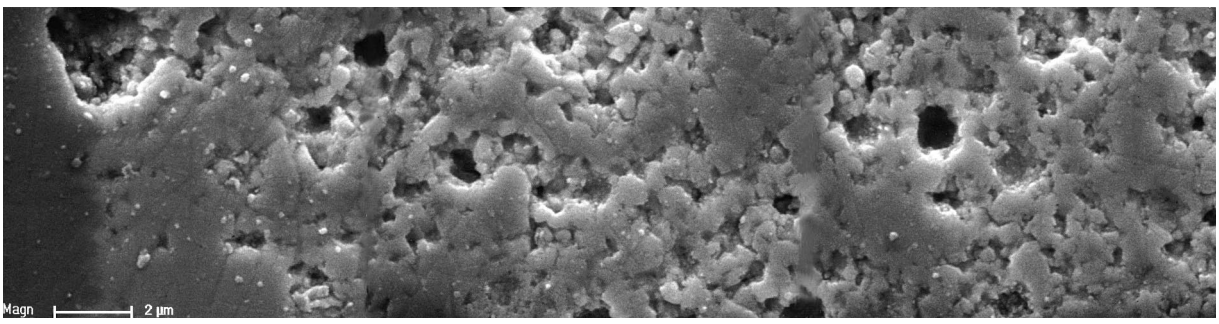

Fig. 10. Fuel to clad contact area, rim on the right and internal zirconia on the left.

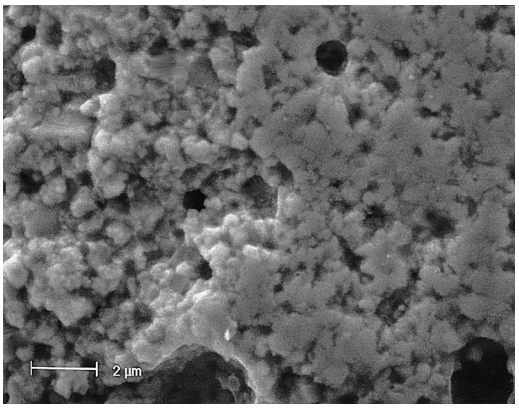

Fig. 11. Polished fuel and fractured fuel interface: same polished rim as in Fig. 4 (left part) and rim microstructure illustration (right part).

penetration between fuel and internal zirconia is illustrated. These different morphologies exhibit the contact zone heterogeneous behaviour.

The compact zone between fuel and cladding has a different morphology and behaviour compared to the material damaged by the rim effect. Microprobe chemical analysis shows that in some of these areas, fission product concentrations are not correlated to U and Pu fission. Some fission products are implanted in the cladding, as illustrated in Fig. 1. Consequently, the peripheral Nd depletion resembles a burnup decrease at the pellet edge. In the five last micrometers, the material has less fission products and then crystallographic defects than in the other parts of the rim. This peripheral area seems to be undamaged. This observation suggests that a composition effect and/or a flux of fission product effect has a dramatic influence on the rim effect.

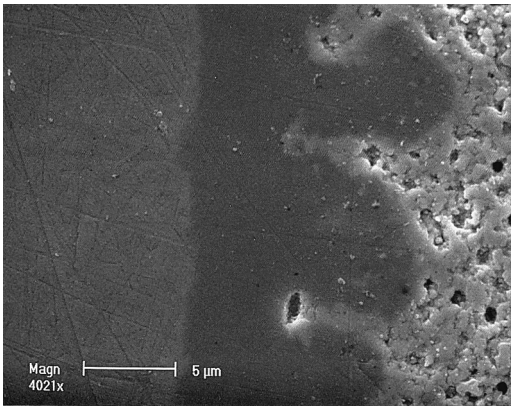

Fig. 12. Fuel to clad contact area, rim and internal zirconia important interpenetration. Cladding on the left, fuel on the right.

6. Subgrain formation mechanisms

6.1. Literature review

The rim phenomenon seems to be linked to defect accumulation in the material. But no definitive mechanism has been established for the grain subdivision characteristic of rim effect.

Among the various models, Matzke [1] suggests that overpressurized bubbles are at the origin of fragmentation. To emphasise this hypothesis, a simulation by Xe implantation was performed. However the subgrain morphology obtained by Xe implantation corresponds more to round subgrains than to rim effect. Thomas et al. [7] use the metallurgist notion of recrystallization to describe the rim effect. This interpretation is in contradiction with the very small mismatch between subgrains observed by Matzke [13]. TEM observations evidenced plane defects perpendicular to the direction (1 1 1). From TEM observations, Une et al. [14] suggest that tangled dislocation networks can be the origin of subgrains. They show areas with different defect concentrations around coarsened pore [2].

In a recent study, Spino et al. [3] describe the rim effect as a fragmentation mechanism linked to pores. They propose the hypothesis of a subgrain formation around pores, and the subdivision of all initial grains of the rim area. Baron et al. [5] use a mechanism that summarises the two latter interpretations into an original model. In their approach, restructuring propagates around stabilised porosities able to trap atoms and vacancies, of which diffusion is enhanced by the numerous crystallographic defects. These interpretations could correspond to a surface rearrangement mechanism, and explain polyhedral subgrains formed by dislocation walls. But, even if pore formation was described, there is no further explanation about their location: intergranular at first, and intragranular closer to the pellet edge.

Our present observations highlight the coexistence of two types of granularities in the rim area. The existence of these types of granularity implies a new difficulty in understanding the rim effect. Subgrain existence should not be the only criterion to assess the existence of the rim effect. According to our observations, only polyhedral subgrain appearance should be considered as characteristic of the rim effect, which should be more appropriately called subdivision effect as proposed in [2,7]. This is of major importance when considering rim width, because round grains can be found in a much wider area than polyhedral grains. Small round subgrains around small pores have already been observed on the rim area of a Risöe fuel pellet, this result has been interpreted as a rim effect [15]. Our study tends to prove that a more thorough analysis is needed to obtain a better understanding of the rim effect.

Our observations pointed out two subgrains morphologies. We assume that these two subgrains formation could correspond to two different mechanisms.

In the following paragraphs, base elements for mechanism are presented.

6.2. Rim formation

Rim is characterised by the appearance of micronics pores, the subdivision of initial grains onto polyhedral subgrains and the xenon depletion. Pores are intergranular in the rim vicinity and intragranular closer to the pellet edge and sticks increase in the rim vicinity have been evidenced. The mechanism to explain the rim formation should highlight the relation between these elements. We have already shown that planar defect could explain the polyhedral shape of the rim subgrains, and the existence of a relation between pore formation and gas release. The next proposition is made: The planar defects could be accompanied by gas release, and should be preferential sites for pores formation. In the rim vicinity released gas could be resoluted in the bulk grain because of the planar defect stickness, while at the grain boundary gas diffusion is enhanced and pore formation is allowed. In the rim itself, the plate defect density is higher creating polyhedral subgrains and intragranular pores due to planar defect crossover.

To validate these assumptions further characterisations of sticks are needed to better understand their formation (defect accumulation as dislocation loop), their crystallographic orientation and to determine their content.

6.3. Free surface rearrangement

Round subgrains are associated to open surfaces, bottom of a fabrication pore for example. This original feature could be explained by the physic of free surface under irradiation. Turos et al. [11] have shown by TEM analysis that fission fragments eliminate nanometer pores, assuming that fission fragments carry away atoms that fulfil small pores. A flux of fission products could then modify grain surfaces inside a pore. Hocking et al. [10] mcasured by X-ray photoelectron spectroscopy (XPS) a composition difference on the fragmented CANDU fuel described above. Moreover, Ingo et al. [17] demonstrate by XPS analysis that the irradiation of Y_2O_3–Z_rO_2 with Ar^0 induces Zr and Y reduction and segregation to the surface. According to these observations, fission fragment movement through an open surface could induce a concentration difference between the bulk and the open surface of grains and, as a consequence, a surface rearrangement. By calculation and surface characterisation, Mullins [18] shows that the thermodynamic equilibrium shape of grain boundaries is round. These elements could explain rolls and ordered subgrain formation at the open surface of the initial grain. More EPMA studies are needed onto free surfaces showing different morphologies.

7. Conclusion

The results presented in this paper give two new important items of information on rim. First two types of subgrains are observed in rim area: polyhedral subgrains which are characteristic of rim effect and round subgrains which seem to be correlated free surface rearrangement inside a pore. That is why, in our opinion, a careful examination of subgrains should be performed before assigning any width to the rim effect. Round subgrain formation due to surface rearrangements can be compared to the appearance of subgrains around pores as proposed by Spino et al. [3]. Recently, Matzke [19] observed round subgrains in other irradiated materials as $MgAl_2O_4$, and proposed a common mechanism called polygonization. According to our interpretation, this should not be associated to the rim effect. Second, two specific defects are observed in fuel grain in the vicinity of rim area: planar defects and small intergranular pores. These defects can be considered as precursor of rim effect because their density increases when approaching pellet edge. A mechanism is proposed in which planar defect have a major influence. This mechanism emphasises the defect concentration in the rim area as already pointed out by Une [2,16,20], Baron et al. [5], and Hermitte [4].

More observations are needed to refine the proposed mechanisms especially referring to planar defects and small intergranular pores seen in the vicinity of rim area. The results reported in the present paper should be considered as a first stimulus to further investigations on the rim microstructure, and as new data to understand rim formation mechanism.

Acknowledgements

This work has been conducted thanks to the CEA. We would like to thank the CEA for a contract granted to two of us (D.A., J.C.N.). The authors wish to express their gratitude to B. Pasquet and V. Cuisset who performed the EPMA analysis, to I. Rochas who worked on the SEM acquisitions, and to D. Lespiaux, Th. Blay and R. Espitallier who performed ceramographic examinations.

References

[1] Hj. Matzke, A. Turos, G. Linker, Nucl. Instrum. and Meth. B 91 (1994) 294.
[2] K. Une, K. Nogita, S. Kashibe, M. Imamura, J. Nucl. Mater. 188 (1992) 65.
[3] J. Spino, K. Vennix, M. Coquerelle, J. Nucl. Mater. 231 (1996) 179.
[4] B. Hermitte, Etude et modélisation de la physico-chimie du rim dans le combustible des crayons REP, thesis, France, 1996.
[5] D. Baron, B. Hermitte, J.P. Piron, IAEA, Technical Committee Meeting on Advances in Pellet Technology for improved Performance at High Burnup, Tokyo, Japan, 28 Oct.–1 Nov. 1996, Paper no. 3.7.
[6] J. Noirot, to be published.
[7] L.E. Thomas, C.E. Beyer, L.A. Charlot, J. Nucl. Mater. 188 (1992) 80.
[8] S.R. Pati, A.M. Garde, L.J. Clinck, ANS Topical Meeting on LWR Fuel Performance, Williamsburg, Virginia, 17–20 April 1988, pp. 204–215.
[9] Hj. Matzke, J. Nucl. Mater. 208 (1994) 18.
[10] W.H. Hocking, A.M. Duclos, L.H. Johnson, J. Nucl. Mater. 209 (1994) 1.
[11] A. Turos, Hj. Matzke, Nucl. Instrum. and Meth. B 65 (1992) 315.
[12] T.J. Carter, I.J. Hastings, A.D. Smith, G.C. Miller, I.A. Lusk, R.E. Moeller, D.H. Rose, Internal Topical Meeting on LWR Fuel Performance, Avignon, France, 21–24 April 1991, pp. 818–827.
[13] Hj. Matzke, L.M. Wang, J. Nucl. Mater. 231 (1996) 155.
[14] J.A. Turnbull, M.D. Freshley, D.D. Lanning, J. Nucl. Mater. 107 (1982) 168.
[15] I.L.F. Ray, Hj. Matzke, H.A. Thiele, M. Kinoshita, J. Nucl. Mater. 245 (1997) 115.
[16] K. Nogita, K. Une, J. Nucl. Mater. 226 (1995) 302.
[17] G.M. Ingo, G. Marletta, Nucl. Instrum. and Meth. B 116 (1996) 440.
[18] W.W. Mullins, J. Appl. Phys. 28 (1957) 333.
[19] Hj. Matzke, M. Kinoshita, J. Nucl. Mater. 247 (1997) 108.
[20] K. Une, K. Nogita, S. Kashibe, T. Toyanga, M. Amaga, International Topical Meeting on Light Water Reactor fuel performances, Portland, Oregon, 2–6 March 1997.